IEEE Access
Multidisciplinary | Rapid Review | Open Access Journal

SPECIAL SECTION ON EMERGING TRENDS, ISSUES, AND CHALLENGES IN ENERGY-EFFICIENT CLOUD COMPUTING

Received January 4, 2017, accepted January 15, 2017, date of publication February 13, 2017, date of current version March 13, 2017.

Digital Object Identifier 10.1109/ACCESS.2017.2667678

Energy-Efficient Sub-Carrier and Power Allocation in Cloud-Based Cellular Network With Ambient RF Energy Harvesting

YISHENG ZHAO[1,2], (Member, IEEE), VICTOR C. M. LEUNG[2], (Fellow, IEEE), CHUNSHENG ZHU[2], (Member, IEEE), HUI GAO[3], (Senior Member, IEEE), ZHONGHUI CHEN[1], AND HONG JI[4], (Senior Member, IEEE)

[1]College of Physics and Information Engineering, Fuzhou University, Fuzhou 350108, China
[2]Department of Electrical and Computer Engineering, The University of British Columbia, Vancouver, BC V6T 1Z4, Canada
[3]School of Information and Communication Engineering, Beijing University of Posts and Telecommunications, Beijing 100876, China
[4]Key Laboratory of Universal Wireless Communications, Ministry of Education, Beijing University of Posts and Telecommunications, Beijing 100876, China

Corresponding author: C. Zhu (cszhu@ece.ubc.ca)

This work was supported in part by the National Natural Science Foundation of China under Grant U1405251, Grant 61401041, Grant 61571129, Grant 61601126, and Grant 61671088, in part by the Natural Science Foundation of Fujian Province under Grant 2015J05122 and Grant 2015J01250, in part by the Canadian Natural Sciences and Engineering Research Council, and in part by the China Scholarship Council (CSC).

ABSTRACT Due to the limited battery energy of mobile devices, the issue of energy-efficient resource allocation has drawn significant interest in the mobile cloud computing area. Simultaneous wireless information and power transfer (SWIPT) is an innovative way to provide electrical energy for mobile devices. Extensive research on the resource allocation problem is conducted in SWIPT systems. However, most previous works mainly focus on energy harvesting over a relatively narrow frequency range. Due to small amounts of energy harvested by the users, the practical implementations are usually limited to low power devices. In this paper, an energy-efficient uplink resource allocation problem is investigated in a cloud-based cellular network with ambient radio frequency (RF) energy harvesting. In order to obtain sufficient energy, a broadband rectenna is equipped at the user device to harvest ambient RF energy over six frequency bands at the same time. From the viewpoint of service arrival in the ambient transmitter, a new energy arrival model is presented. The joint problem of sub-carrier and power allocation is formulated as a mixed-integer nonlinear programming problem. The objective is to maximize the energy efficiency while satisfying the energy consumption constraint and the total data rate requirement. In order to reduce the computational complexity, a suboptimal solution to the optimization problem is derived by employing a quantum-behaved particle swarm optimization (QPSO) algorithm. Simulation results show that more energy can be harvested by the user devices compared with narrow band SWIFT systems, and the QPSO method achieves higher energy efficiency than a conventional particle swarm optimization approach.

INDEX TERMS Ambient RF energy harvesting, cloud-based cellular network, energy efficiency, resource allocation.

I. INTRODUCTION

With the wide popularity of smart mobile devices, mobile cloud computing [1]–[4] has become a new service model. Mobile devices can be implemented without complex hardware and software, but instead use the abundant resources available from cloud computing platforms. However, one of the most challenging problems for mobile devices is the limited battery energy [5]–[7]. The energy consumption problem [8], [9] has attracted great attention. Therefore, how to design an energy-efficient resource allocation strategy to prolong the battery life of mobile devices [5], [10] is of great importance to improve the system utility.

Radio frequency (RF) energy harvesting is an emerging solution to provide electrical energy for mobile equipments. The user devices can harvest energy from the received electromagnetic waves. The RF sources can mainly be divided into two categories, including dedicated RF sources and ambient RF sources. For the former, the dedicated

2169-3536 © 2017 IEEE. Translations and content mining are permitted for academic research only.
Personal use is also permitted, but republication/redistribution requires IEEE permission.
See http://www.ieee.org/publications_standards/publications/rights/index.html for more information.

transmitters (e.g., power beacons [11] and hybrid access point [12]) broadcast only energy to user devices. For the latter, the RF signals radiated by the ambient transmitter carry both information and power at the same time, which is called simultaneous wireless information and power transfer (SWIPT) [13].

From the perspective of SWIPT, many previous works [14]–[17] have considered the resource allocation strategies to improve the system performance. In [14], both continuous and discrete power splitting ratios were taken into account in the receivers to harvest energy. The problems of downlink sub-carrier and power allocation were investigated to maximize the energy efficiency in Wi-Fi systems. By employing the fractional programming and the dual decomposition, suboptimal iterative algorithms were developed to solve the non-convex optimization problems. C. Xiong *et al.* [15] discussed the downlink and uplink energy efficiency tradeoff in the scenarios with one access point (AP) and multiple users. The users were able to split the received signals for information decoding and energy harvesting in the downlink. The established integer-mixed optimization problem was solved through relaxation and transformation. In [16], the downlink multi-user scheduling was studied in the SWIPT systems with one AP and multiple users. When one user was scheduled for information transmission, other idle users could harvest energy from the received signal. Novel order-based scheduling schemes were proposed to control the tradeoff between the users' rates and their average amount of harvested energy. A SWIPT system with a transmitter equipped with multiple antennas serving two information receivers and multiple energy harvesting receivers was considered in [17]. The objective was to maximize the total harvested energy at energy harvesting receivers subject to minimum required signal-to-interference-plus-noise ratios at the information receivers. The formulated non-convex optimization problem was optimally solved by an iterative algorithm.

However, these existing works mostly focus on energy harvesting over a relatively narrow frequency range. The frequency bands considered in [14]–[17] are 470 MHz, 800 MHz, 915 MHz, and 915 MHz. The corresponding system bandwidths are 20 MHz, 960 kHz, 26 MHz, and 200 kHz, respectively. Due to the limited RF sources, the total amount of energy harvested by the users is small. The average harvested power is about 12 dBm (i.e., 15.8 mW) [14], 0.1 mW [16], and -5 dBm (i.e., 0.3 mW) [17], respectively. The practical implementations will be limited to low power devices such as wireless sensor nodes, radio frequency identification (RFID) tags, and so on. It is well known that there are all kinds of electromagnetic emissions spanning a much wider frequency bandwidth in the air. Intuitively, if the user device can harvest energy over a broad frequency range, more energy will be harvested, and a much wider variety of devices can benefit from ambient RF energy harvesting. The main challenge of this approach, i.e., the design an appropriate antenna to capture broadband ambient RF signals, has been addressed by recent advances in antenna techniques.

An efficient rectenna (i.e., rectifying antenna) array [18], [19] was designed to harvest ambient RF energy over a broad bandwidth. Although the antenna array is effective in energy harvesting, the drawback is that the size of the antenna array is usually large. Therefore, the antenna array is not suitable for user devices in the cellular network. Another antenna technique is designing broadband antenna, which can harvest energy from multiple frequency bands simultaneously. Dual-band [20], triple-band [21], [22], and four-band [23] antennas were designed to harvest energy from different frequency bands. In addition, a novel broadband dual circular polarization receiving antenna was reported in [24]. The proposed rectenna could cover six frequency bands, including digital television (DTV) channel (550-600 MHz), Long Term Evolution (LTE, 750-800 MHz), Global System for Mobile communications (GSM900, 850-910 MHz), GSM1800 (1850-1900 MHz), Universal Mobile Telecommunications System (UMTS, 2150-2200 MHz), and Wi-Fi (2.4-2.45 GHz).

In addition, some prior works have been done to analyze the performance of a wireless sensor node powered by ambient RF energy harvesting. A point-to-point uplink transmission between an RF-powered sensor node and a data sink was considered in [25]. A point-to-point downlink SWIPT transmission from an AP to an RF-powered sensor node was considered in [26]. The problem of resource allocation [27] was discussed in wireless network with RF energy harvesting. A case study of a receiver operation policy was presented in the scenario of a node and an AP. To the best of our knowledge, the resource allocation issue of multiple users in a cloud-based cellular network with ambient RF energy harvesting has not been investigated in the literature. Moreover, for the optimization problem of resource allocation, it is usually hard to obtain an optimal solution with low computational complexity. Quantum-behaved particle swarm optimization (QPSO) [28]–[31] is a kind of swarm intelligence algorithm, which is fit to solve the complicated optimization problem. A suboptimal solution can be achieved at relatively low cost.

Motivated by the above observations, we propose a novel energy-efficient uplink sub-carrier and power allocation strategy by using the QPSO algorithm in a cloud-based cellular network with ambient RF energy harvesting. The distinct features of this paper are summarized as follows:

- A multi-user resource allocation strategy in the cloud-based cellular network with broadband RF energy harvesting is proposed for the first time. Different from the work [14] in Wi-Fi systems with energy harvesting over a relatively narrow frequency band, a novel uplink sub-carrier and power allocation strategy is developed in the cloud-based cellular network with multiple users. Equipped with a broadband antenna, each user can harvest energy from multiple ambient RF sources. The objective is to maximize the energy efficiency under the

TABLE 1. Main symbols and meanings.

Symbols	Meanings
E_k^H	Energy harvested by the k-th user
E_k^{H1}	Energy harvested from the TV towers by the k-th user
E_k^{H2}	Energy harvested from the dynamic ambient RF sources by the k-th user
P_l^{TV}	Transmission power of the l-th TV tower
G_l^{TV}	Transmission antenna gain of the l-th TV tower
G_k^R	Receive antenna gain of the k-th user
$d_{k,l}^{TV}$	Distance between the k-th user and the l-th TV tower
f_l^{TV}	Transmission frequency of the l-th TV tower
$E_{k,i}^{H2}$	Energy harvested from the i-th ambient transmitter by the k-th user
P_i^T	Transmission power of the i-th ambient transmitter
G_i^T	Transmission antenna gain of the i-th ambient transmitter
$d_{k,i}$	Distance between the k-th user and the i-th ambient transmitter
$f_{i,j}$	Frequency of the j-th service for the i-th ambient transmitter
$t_{i,j}$	Arrival time of the j-th service for the i-th ambient transmitter
$T_{i,j}^S$	Average service time of the j-th service for the i-th ambient transmitter
R_{total}	Total data rate
T_{dt}	Duration of data transmission
D_{total}	Amount of total data transmitted by the users
E_{total}	Total energy consumption
$\mathbf{X}_m(s)$	Position of the m-th particle in the s-th iteration
$\mathbf{C}(s)$	Mean best position of all the particles in the s-th iteration
$\mathbf{P}_m(s)$	Local best position of the m-th particle in the s-th iteration
$\mathbf{G}(s)$	Global best position of all the particles in the s-th iteration

constraints of energy consumption and total data rate requirement.

- From the perspective of service arrival in the ambient transmitter, a new energy arrival model is presented. In the previous works [25], [26], the location distribution of the ambient RF transmitters is modeled by adopting a Ginibre α-determinantal point process. It is assumed that the transmission power of each ambient transmitter is the same. Different from the above method, we suppose that the location of the ambient transmitters is fixed while the transmission power, the service arrival, and the service time of each ambient transmitter are variable, which is more practical.
- An improved QPSO algorithm is used to solve the formulated resource allocation optimization problem. In a previous work [31], each user in the network is regarded as a particle, resulting in the same resource allocation for different users, which is not reasonable in practical systems. In contrast, we modify the definition of the particle by including the resource allocation parameters of all the users in the definition of the particle position. Thus, a particle is composed of all the users in the network, which is conducive to obtain a reasonable suboptimal solution.

The rest of the paper is organized as follows. In Section II, the system description is presented. The problem formulation and solution are presented and analyzed in Section III. Simulation results and discussions are shown in Section IV. Finally, conclusions and future work are given in Section V.

There are many symbols in this paper. For the readers' convenience, the main symbols and their meanings are listed in Table I.

II. SYSTEM DESCRIPTION

In this section, we first introduce the network model with ambient RF energy harvesting. Then, we present the energy arrival model.

A. NETWORK MODEL

As shown in Fig. 1, we consider a communication scenario with one base station (BS) and multiple users in a cloud-based cellular network with ambient RF energy harvesting. The BS is provided with electrical energy by the traditional power grid. It is supposed that there are K users in the network. Each user is equipped with an energy harvesting equipment to harvest energy from the electromagnetic wave in the surrounding environment. In order to obtain sufficient energy, the users harvest energy over a broad frequency range. This is feasible using, e.g., the novel broadband rectenna reported recently in [24], which can harvest energy from six frequency bands at the same time. Following [24], DTV (550-600 MHz), LTE (750-800 MHz), GSM900 (850-910 MHz), GSM1800 (1850-1900 MHz), UMTS (2150-2200 MHz), and Wi-Fi (2.4-2.45 GHz) are considered as the ambient RF sources. The corresponding transmitters are TV tower, eNode B, BS 1, BS 2, Node B, and AP, respectively. In addition, a cloud computing platform is used to provide computing services for user devices. First, the user devices are connected to the BS. They can send data to the BS, which in turn forward the data

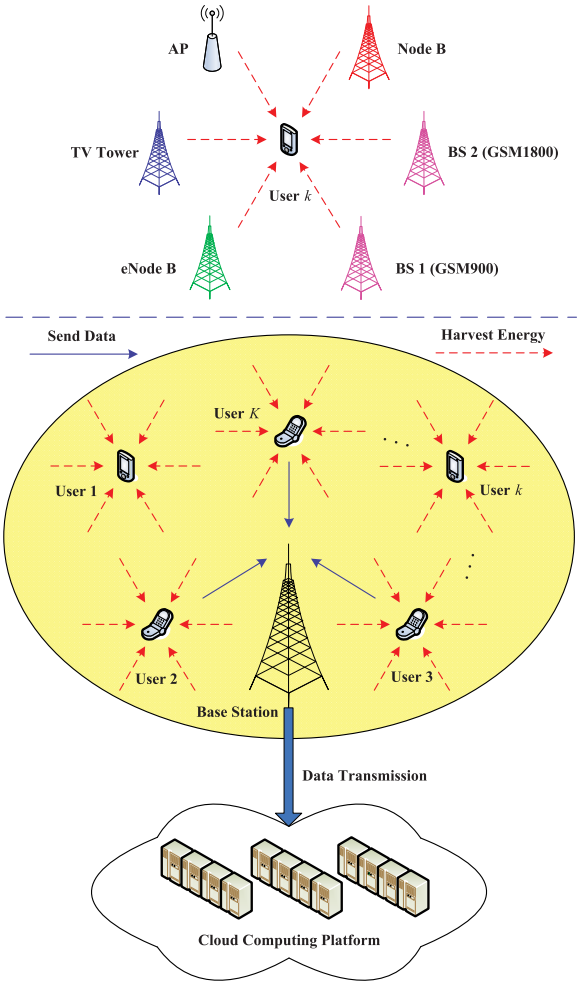

FIGURE 1. Communication scenario of cloud-based cellular network with ambient RF energy harvesting.

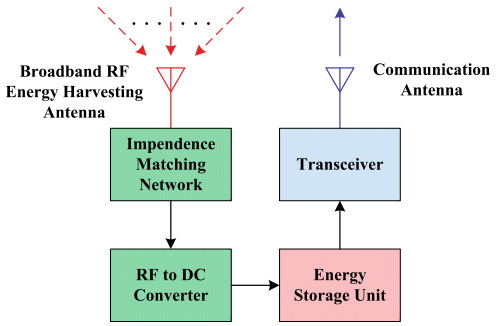

FIGURE 2. General architecture of user device with broadband RF energy harvesting antenna and communication antenna.

to the cloud computing platform through the Internet. The user devices receive data from the cloud computing platform over the same path in the opposite direction.

As illustrated in Fig. 2, the general architecture of the user device consists of three modules. The first one is an energy harvesting module. It consists of a broadband RF energy harvesting antenna, an impendence matching network, and an RF to direct current (DC) converter. The broadband RF energy harvesting antenna is used to harvest energy from the ambient RF signals. The impedance matching network is a resonator circuit, which is utilized to maximize the power transfer between the broadband RF energy harvesting antenna and the RF to DC converter. The RF to DC converter is a rectifying circuit, which converts RF signals into DC voltage. The second module is an energy storage unit (e.g., a rechargeable battery), which is utilized to store the electricity converted by the RF to DC converter. Different from the sensor node, the user device will consume more electrical energy in the cellular network. For instance, the maximum transmission power of user equipment is 23 dBm (i.e., 199.5 mW) in the LTE network [32]. Therefore, to enable storage of sufficient electrical energy, a large capacity battery is needed. The third one is a communication module that is comprised of a transceiver and a communication antenna. The communication antenna is used to send or receive data to or from the BS. Note that in this paper we ignore the energy that can be harvested by a device's broadband RF energy harvesting antenna from its own transmissions. Also, different from conventional SWIPT system models, we consider that the broadband RF energy harvesting antenna and the communication antenna are independent units. Therefore, the user device is able to harvest energy and send data concurrently. Additionally, we assume that the cloud-based cellular network adopts orthogonal frequency-division multiplexing (OFDM) technology in its physical layer. Thus, multiple users can communicate with the BS on the different sub-carriers at the same time.

B. ENERGY ARRIVAL MODEL

In this subsection, the energy arrival model of ambient RF energy harvesting is presented. The Friis equation [33] was employed to construct the energy arrival model in the existing literatures [25], [26]. The location distribution of the ambient RF transmitters was modeled as a Ginibre α-determinantal point process. The effect of the locations of ambient RF sources on the performance of the sensor node was analyzed. For convenience of analysis, the related parameters of different ambient transmitters (e.g., the transmission power, the transmission antenna gain, and the wavelength) were assumed to be the same. Different from the previous works in [25] and [26], a new energy arrival model is designed from the perspective of service arrival in each ambient transmitter in this paper. In the practical communication scenarios, the BS or the AP is usually deployed at a specific location. Therefore, we suppose that the locations of the ambient transmitters are fixed. Furthermore, different classes of ambient transmitters have different transmission power, which should be considered in the energy arrival model. Meanwhile, the service arrival and the average service time are also different for different ambient transmitters.

Note that ambient RF sources can be classified into static and dynamic ambient RF sources [34]. For the first one, the ambient transmitter (e.g., TV tower) transmits power persistently. For the second one, the ambient transmitters

(e.g., BS, Node B, eNode B, and AP) transmit power at intervals, which depends on service arrivals at the downlink. For the static ambient RF sources, L TV towers are considered. For the dynamic ambient RF sources, it is assumed that there are I ambient transmitters. For the k-th user in the cloud-based cellular network with ambient RF energy harvesting, the harvested energy can be denoted by

$$E_k^H = E_k^{H1} + E_k^{H2} \tag{1}$$

where E_k^{H1} and E_k^{H2} indicate the energy harvested from the TV towers and the dynamic ambient RF sources, respectively. Inspired by the Friis equation[1] [33], the energy arrival model of E_k^{H1} is shown as

$$E_k^{H1} = \sum_{l=1}^{L} \frac{P_l^{TV} G_l^{TV} G_k^R c^2}{\left(4\pi d_{k,l}^{TV} f_l^{TV}\right)^2} T\eta \tag{2}$$

where P_l^{TV} and G_l^{TV} are the transmission power and the transmission antenna gain of the l-th TV tower, G_k^R denotes the receive antenna gain of the k-th user, c is the speed of electromagnetic wave propagation in free space, $d_{k,l}^{TV}$ indicates the distance between the k-th user and the l-th TV tower, and f_l^{TV} is the transmission frequency of the l-th TV tower. Moreover, T indicates the duration of harvesting energy and η represents the energy harvesting efficiency of the user device.

Similarly, according to the Friis equation, the energy arrival model of E_k^{H2} is expressed as

$$E_k^{H2} = \sum_{i=1}^{I} E_{k,i}^{H2} \tag{3}$$

where $E_{k,i}^{H2}$ represents the energy harvested from the i-th ambient transmitter by the k-th user. For the i-th ambient transmitter, according to service arrival of downlink, the transmitter transmits power dynamically. The specific expression of $E_{k,i}^{H2}$ is shown as

$$E_{k,i}^{H2} = \sum_{j=1}^{J} \frac{P_i^T G_i^T G_k^R c^2}{\left(4\pi d_{k,i} f_{i,j}\right)^2} B\left(t_{i,j} + T_{i,j}^S \le T\right) T_{i,j}^S \eta \tag{4}$$

where J is the total number of different services, P_i^T and G_i^T indicate the transmission power and the transmission antenna gain of the i-th ambient transmitter, $d_{k,i}$ denotes the distance between the k-th user and the i-th ambient transmitter, and $f_{i,j}$ is the frequency of the j-th service for the i-th ambient transmitter. Additionally, $t_{i,j}$ and $T_{i,j}^S$ denote the arrival time and the average service time of the j-th service for the i-th ambient transmitter. The function $B(\xi)$ is a binary function: the value of $B(\xi)$ is 1 if the condition ξ is true, and 0 otherwise. In other words, for a certain service, only if the arrival time plus the average service time is no greater than the given time T can the user harvest energy from the ambient transmitter. An explanation to the duration of harvesting energy is illustrated in Fig. 3. If $t_{i,j} + T_{i,j}^S \le T$, the duration of harvesting energy is $T_{i,j}^S$. If $t_{i,j} + T_{i,j}^S > T$, the duration of harvesting energy is $T - t_{i,j}$. Usually, $T - t_{i,j}$ is short, which is ignored in this paper. As a consequence, the duration of harvesting energy is equal to the average service time.

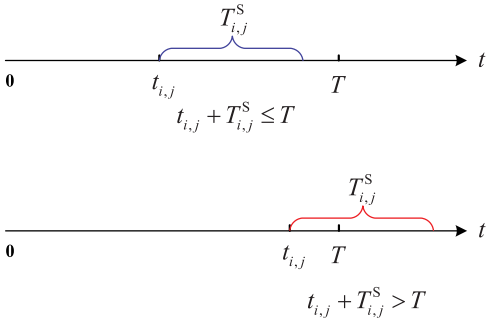

FIGURE 3. Explanation to duration of harvesting energy.

Following [35], a Poisson process is used to describe the service arrivals, while the service time is assumed to follow an exponential distribution. For the i-th ambient transmitter, it is supposed that the average service arrival rate is λ_i. According to the property of Poisson processes, the interarrival time between two consecutive service arrivals, i.e., $t_{i,j+1} - t_{i,j}$, is exponentially distributed with mean $\frac{1}{\lambda_i}$. In addition, for the j-th service of the i-th ambient transmitter, it is assumed that the average service time $T_{i,j}^S$ follows an exponential distribution with mean μ_i.

III. PROBLEM FORMULATION AND SOLUTION

In this section, the formulation of the resource allocation problem is given first. Then, a suboptimal solution to the formulated resource allocation problem is developed. Finally, the complexity analysis is presented.

A. PROBLEM FORMULATION

An energy-efficient uplink sub-carrier and power allocation problem is investigated in the above cloud-based cellular network with ambient RF energy harvesting. It is assumed that K users send data to the BS on N sub-carriers. Usually, N is larger than K. It is assumed that only one user can communicate with the BS on the n-th sub-carrier: this mapping is denoted by the binary variable $\delta_{k,n} \in \{0, 1\}$. In addition, $p_{k,n}$ indicates the transmission power of the k-th user on the n-th sub-carrier. The total data rate can be obtained by

$$R_{total} = \sum_{k=1}^{K} \sum_{n=1}^{N} \delta_{k,n} W \log_2 \left(1 + \frac{p_{k,n} h_{k,n}^2}{N_0 W}\right) \tag{5}$$

where W is the sub-carrier bandwidth, $h_{k,n}$ denotes the channel gain of the k-th user on the n-th sub-carrier, and N_0 represents the power spectral density of additive white Gaussian noise. The unit of the total data rate is bits per second (bits/s). It is assumed that the duration of data transmission is T_{dt}.

[1]Note that only large scale fading is considered in the Friis equation, while small scale fading is ignored.

Thus, the amount of total data transmitted by the users is

$$D_{total} = T_{dt} R_{total}. \tag{6}$$

The unit of D_{total} is bits. At the same time, the total energy consumption [36] is shown as

$$E_{total} = T_{dt} \left(K P_C + \sum_{k=1}^{K} \sum_{n=1}^{N} \delta_{k,n} p_{k,n} \right) \tag{7}$$

where P_C denotes the circuit power consumption of each user. The unit of E_{total} is Joule (J).

The objective of sub-carrier and power allocation problem is to maximize the energy efficiency [37] while satisfying several constraints. This is an optimization problem, which can be formulated as

$$\underset{\delta_{k,n}, p_{k,n}}{maximize} \frac{D_{total}}{E_{total}} \tag{8a}$$

subject to

$$C1: T_{dt} \left(P_C + \sum_{n=1}^{N} \delta_{k,n} p_{k,n} \right) \leq E_k^H, \quad \forall k \tag{8b}$$

$$C2: \sum_{k=1}^{K} \sum_{n=1}^{N} \delta_{k,n} W \log_2 \left(1 + \frac{p_{k,n} h_{k,n}^2}{N_0 W} \right) \geq R_{total}^{\min} \tag{8c}$$

$$C3: \delta_{k,n} \in \{0, 1\}, \quad \forall k, n \tag{8d}$$

$$C4: \sum_{k=1}^{K} \delta_{k,n} = 1, \quad \forall n \tag{8e}$$

$$C5: p_{k,n} \geq 0, \quad \forall k, n \tag{8f}$$

where the objective function is the energy efficiency and its unit is bits per Joule (bits/J). For the k-th user, the first constraint ensures that the harvested energy is no less than the energy consumption, which is called the energy causality. The second constraint guarantees that the total data rate is greater than or equal to the minimum value $R_{total}^{\min}$. The third and fourth constraints show that the n-th sub-carrier can only be allocated to one user. The fifth constraint indicates that the transmission power of the user device is non-negative. Note that the objective function is nonlinear, and the values of $\delta_{k,n}$ and $p_{k,n}$ are, respectively, discrete and continuous. As a consequence, the above optimization problem is a mixed-integer nonlinear programming (MINLP) problem.

B. SUBOPTIMAL SOLUTION

It is quite difficult to obtain a globally optimal solution of the MINLP problem (8) with a low computational complexity. Therefore, a heuristic algorithm is used to derive a suboptimal solution with an acceptable complexity. The QPSO algorithm [28], [30] is a kind of swarm intelligence algorithm, which is suitable to solve the complicated optimization problem. The QPSO algorithm is an improved version of the traditional particle swarm optimization (PSO) algorithm. Consequently, the basic principle of the PSO algorithm will be introduced first.

The basic principle of the standard PSO algorithm is described as follows. Inspired by the social behavior of a flock of bird or a school of fish, the PSO algorithm was developed by J. Kennedy *et al.* [38], [39] to solve the optimization problem. It is assumed that there are particles in the multi-dimensional space. For the m-th ($m = 1, 2, ..., M$) particle, its position vector X_m and velocity vector V_m are defined. Each particle can be evaluated by a fitness function. The movement of each particle is guided by its local best position P_m and a global best position G. The velocity and position of each particle [40] are updated by the following iterative equations

$$\begin{cases} V_m(s+1) = \omega V_m(s) + c_1 r_1 (P_m - X_m(s)) \\ \qquad\qquad + c_2 r_2 (G - X_m(s)) \\ X_m(s+1) = X_m(s) + V_m(s+1) \end{cases} \tag{9}$$

where s denotes the iteration number, ω indicates the inertia weight, c_1 and c_2 are two constants called the acceleration coefficients, and r_1 and r_2 are random numbers between 0 and 1. When the iteration number is equal to the maximum iteration number S, the iteration is terminated. However, the PSO algorithm can easily converge to a locally optimal solution. Therefore, it is necessary to develop an improved algorithm that can avoid the local search. The QPSO algorithm can overcome the disadvantage of the PSO algorithm and obtain a suboptimal solution that is close to globally optimal.

From the perspective of quantum theory, the particle is considered as a quantum particle. According to the uncertainty principle [41], the exact values of the position and the velocity cannot be determined simultaneously. As a consequence, only the position vector X_m ($m = 1, 2, ..., M$) is defined in the QPSO algorithm. For the m-th particle, the position is updated based on the following iterative equation

$$X_m(s+1) = P \pm \beta \left| C(s) - X_m(s) \right| \cdot \ln (1/u) \tag{10}$$

where β is the contraction-expansion coefficient, u is a random number between 0 and 1, and $C(s)$ is the mean best position of all the particles in the s-th iteration. Moreover, the vector P is given by

$$P = \varphi P_m(s) + (1 - \varphi) G(s) \tag{11}$$

where φ is a random number between 0 and 1, $P_m(s)$ is the local best position of the m-th particle in the s-th iteration, and $G(s)$ denotes the global best position of all the particles in the s-th iteration.

In order to apply the QPSO algorithm to solve the MINLP problem in (8), the original constrained optimization problem needs to be transformed to an unconstrained form, which can be done by the penalty function method. Thus, a fitness function that consists of one objective function and one penalty function is constructed as

$$F\left(\delta_{k,n}, p_{k,n}\right) = f_{obj}\left(\delta_{k,n}, p_{k,n}\right) - \gamma P_f\left(\delta_{k,n}, p_{k,n}\right) \tag{12}$$

where $f_{obj}\left(\delta_{k,n}, p_{k,n}\right)$ is the objective function in (8), γ denotes the penalty factor, and $P_f\left(\delta_{k,n}, p_{k,n}\right)$ indicates the

penalty function that includes five items

$$P_f\left(\delta_{k,n}, p_{k,n}\right) = P_f^1 + P_f^2 + P_f^3 + P_f^4 + P_f^5. \tag{13}$$

They correspond to the five constraints of the optimization problem in (8), which are shown as

$$P_f^1 = \sum_{k=1}^{K}\left[\max\left(0, T_{dt}\left(P_C + \sum_{n=1}^{N}\delta_{k,n}p_{k,n}\right) - E_k^H\right)\right]^2 \tag{14a}$$

$$P_f^2 = \left[\max\left(0, A\right)\right]^2 \tag{14b}$$

$$P_f^3 = \sum_{k=1}^{K}\sum_{n=1}^{N}\left(\delta_{k,n}^2 - \delta_{k,n}\right)^2 \tag{14c}$$

$$P_f^4 = \sum_{n=1}^{N}\left(\sum_{k=1}^{K}\delta_{k,n} - 1\right)^2 \tag{14d}$$

$$P_f^5 = \sum_{k=1}^{K}\sum_{n=1}^{N}\left[\max\left(0, -p_{k,n}\right)\right]^2 \tag{14e}$$

where $max(\cdot,\cdot)$ returns a greater number between two numbers. In (14b), A is given as

$$A = R_{total}^{\min} - \sum_{k=1}^{K}\sum_{n=1}^{N}\delta_{k,n}W\log_2\left(1 + \frac{p_{k,n}h_{k,n}^2}{N_0 W}\right). \tag{15}$$

The fitness function in (12) will be used to evaluate each particle.

Then, the particle position is defined. In the previous work [31], each user in the network is regarded as a particle. Thus, each particle position is composed of sub-carrier and power allocation parameters of one user. However, there exists a shortcoming under this definition. When the position of each particle is updated, sub-carrier and power allocation results of different users eventually become the same values. Obviously, this is not reasonable in practical systems. Therefore, the definition of the particle position needs to be modified. In this paper, the particle position consists of the sub-carrier and power allocation parameters of K users. For the m-th particle, its position vector X_m can be expressed as

$$X_m = \left(X_m^1, X_m^2, ..., X_m^k, ..., X_m^K\right) \tag{16}$$

where X_m^k denotes the sub-carrier and power allocation result of the k-th user. The specific expression of X_m^k is shown as

$$X_m^k = \left(\delta_{k,1}, \delta_{k,2}, ..., \delta_{k,N}, p_{k,1}, p_{k,2}, ..., p_{k,N}\right). \tag{17}$$

It can be seen that X_m^k is a multi-dimensional vector. The first N elements indicate the sub-carrier allocation result. The remaining N elements denote power allocation result on different sub-carriers.

According to the position update equation in (10), the position of each particle is updated by

$$\begin{cases} X_m(s+1) = P + \beta\left|C(s) - X_m(s)\right| \cdot \ln\left(1/u\right), & r \geq 0.5 \\ X_m(s+1) = P - \beta\left|C(s) - X_m(s)\right| \cdot \ln\left(1/u\right), & r < 0.5 \end{cases} \tag{18}$$

Algorithm 1 Energy-Efficient Sub-Carrier and Power Allocation Strategy Based on QPSO

```
Initialization:
Initialize the particle number M, the maximum iteration number S, and the position of each particle X_m(1) (m = 1, ..., M).
Set P_m(1) = X_m(1) and choose a best position from P_m(1) (m = 1, ..., M) as the global best position G(1) based on (12) and (22).
Iteration:
Set s = 1 and m = 1.
while s ≤ S do
  while m ≤ M do
    Calculate C(s) and P based on (20) and (11).
    Update the particle position based on (18).
    Update P_m(s) based on the fitness function in (12). If F[X_m(s+1)] > F[P_m(s)], then P_m(s+1) = X_m(s+1), otherwise P_m(s+1) = P_m(s).
    Update G(s) based on the fitness function in (12). If F[P_m(s+1)] > F[G(s)], then G(s+1) = P_m(s+1), otherwise G(s+1) = G(s).
  end while
end while
Output:
Calculate the fitness function value in the global best position based on (12) and output the function value.
```

where r is a random number between 0 and 1. The value of β in the s-th iteration can be calculated by

$$\beta = 0.5\frac{S - s}{S} + 0.5 = 1 - \frac{s}{2S}. \tag{19}$$

In addition, the mean best position $C(s)$ can be obtained by

$$C(s) = \frac{1}{M}\sum_{m=1}^{M}P_m(s). \tag{20}$$

Based on the fitness function in (12), the local best position $P_m(s)$ can be derived by

$$P_m(s) = \begin{cases} X_m(s), & F\left[X_m(s)\right] > F\left[P_m(s-1)\right] \\ P_m(s-1), & F\left[X_m(s)\right] \leq F\left[P_m(s-1)\right]. \end{cases} \tag{21}$$

The vector P in (18) is given by (11), in which the global best position $G(s)$ can be obtained by

$$\begin{cases} \varepsilon = \arg\max\limits_{1\leq m\leq M}\left\{F\left[P_m(s)\right]\right\} \\ G(s) = P_\varepsilon(s). \end{cases} \tag{22}$$

In order to clearly illustrate the proposed resource allocation strategy based on QPSO, the detailed steps are shown in **Algorithm 1**.

C. COMPLEXITY ANALYSIS

In this subsection, the computational complexity of **Algorithm 1** is analyzed. The computational complexity is

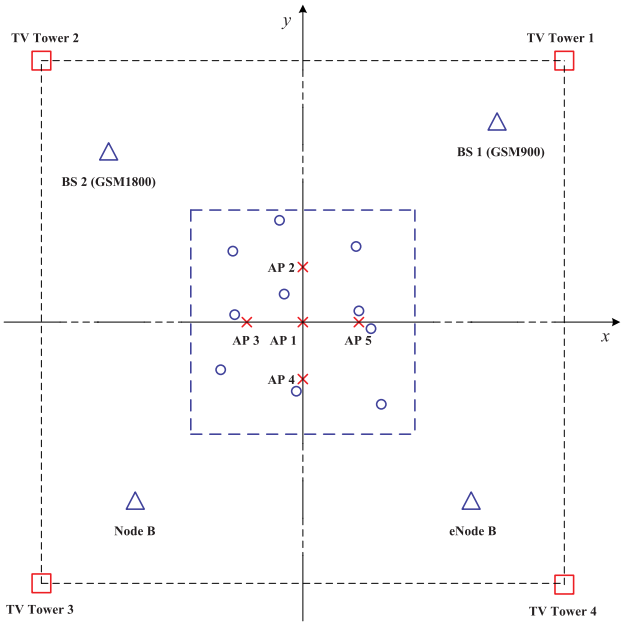

FIGURE 4. Simulation scenario of energy harvesting.

mainly from Line 3 to Line 15. Line 3, which is executed once, has a time complexity of $O(1)$. The specific elapsed time will depend on the function operations in (12) and (22). The time complexity of Line 5 is also $O(1)$. Lines 6-13 consist of two loops: an outer loop and an inner loop. The inner loop given by Lines 8-11 is executed SM times. The time complexity of Lines 6-13 is $O(SM)$. The specific elapsed time will depend on the function operations in (20), (11), (18), and (12). For Line 15, it is also executed one time with time complexity $O(1)$. As a consequence, the total time complexity of **Algorithm 1** is $O(SM)$. In Section IV, a performance metric called average CPU time will be used to evaluate the time complexity.

IV. SIMULATION RESULTS AND DISCUSSIONS

In this section, the performance of the proposed resource allocation strategy is evaluated by simulations. First, the simulation scenario and the parameter settings are given. Then, the amount of energy harvested by different users is presented. The convergence and time complexity of the QPSO algorithm are discussed in the following subsection. Finally, performance comparisons are shown.

A. SIMULATION SCENARIO AND PARAMETER SETTINGS

In this subsection, the simulation scenario and the parameter settings are presented. In order to highlight multiple ambient RF sources, an urban area scenario in which DTV, GSM900, GSM1800, UMTS, LTE, and Wi-Fi coexist would be appropriate. For convenience, the simulation scenario of energy harvesting is illustrated in Fig. 4. There are four TV towers and five kinds of dynamic ambient transmitters (i.e., BS 1 (GSM900), BS 2 (GSM1800), Node B, eNode B, and AP) in the simulations. One BS 1 (GSM900), one BS 2 (GSM1800), one Node B, one eNode B, and five APs are configured in the simulation scenario. Different users represented by the blue circles in Fig. 4 are randomly distributed in the area indicated by the blue square.

For the energy arrival model, the related parameters are set as follows. A rectangular coordinate system with meter (m) as unit is considered. The coordinates of four TV towers are (2000,2000), (−2000,2000), (−2000,−2000), and (2000,−2000). The coordinates of BS 1, BS 2, Node B, and eNode B are (150,150), (−110,110), (−80,−80), and (80,−80). The coordinates of five APs are (0,0), (0,10), (−10,0), (0,−10), and (10,0). Meanwhile, the transmission power of the TV tower, BS 1, BS 2, Node B, eNode B, and AP are 30 kW, 80 W [42], 40 W [42], 43 dBm (i.e., 20 W) [43], 43 dBm [44], and 20 dBm (i.e., 0.1 W). Their transmission antenna gains are 15 dBi, 18 dBi [45], 18 dBi, 9 dBi, 12 dBi [44], and 10 dBi. For the TV channel, GSM900, GSM1800, UMTS, LTE, and Wi-Fi, the frequency or carrier spacings are 8 MHz, 200 kHz, 200 kHz, 5 MHz, 15 kHz, and 5 MHz. All the users are randomly distributed in the blue square area with the coordinates of its four vertices being (20,20), (−20,20), (−20,−20), and (20,−20). The receive antenna gains of all the users are 0 dBi. In addition, the average service arrival rates of BS 1, BS 2, Node B, eNode B, and AP are 0.1, 0.2, 0.3, 0.3, and 0.1 service arrivals per second. For the service time, the means of the exponential distributions are 200 s, 300 s, 500 s, 600 s, and 900 s. The remaining parameters are set as $c = 3 \times 10^8$ m/s, $T = 2000$ s, and $\eta = 0.6$. For the resource allocation strategy, the related parameters are set as $W = 15$ kHz, $N_0 = 2 \times 10^{-10}$ W/Hz, $T_{dt} = 1$ s, $P_C = 0.3$ W, $\gamma = 1.5$, and $R_{total}^{\min} = 10$ Mbps. Without loss of generality, we assume that the values of different $h_{k,n}$ are generated by random numbers with uniform distribution between 0 and 1.

B. AMOUNT OF ENERGY HARVESTED BY USERS

The amount of energy harvested by different users from different ambient transmitters is presented in Table II. In the simulations, the numbers of users and sub-carriers are set as 10 and 80. It can be seen that the users can harvest more energy from the eNode B and the BS 1 and less energy from the AP and the Node B. This is because the eNode B and the BS 1 have lower operation frequencies than the Node B. Meanwhile, the BS 1 has larger transmission power. Although the distances between the AP and the users are relatively short, the energy harvested by the users from the AP is small because of the low transmission power. For user 3, user 6, user 7, and user 9, they can harvest more energy from the AP 5, AP 3, AP 4, and AP 5. The reason is that user 3, user 6, user 7, and user 9 are very near to the AP 5, AP 3, AP 4, and AP 5. Furthermore, the total energy harvested from all the ambient transmitters is also calculated in Table II. Compared with a single ambient transmitter, each user can harvest more energy from multiple ambient transmitters with different operating frequencies.

TABLE 2. Energy harvested by different users from multiple ambient RF sources (unit: J).

Users	User 1	User 2	User 3	User 4	User 5	User 6	User 7	User 8	User 9	User 10
BS 1	1.9641	1.7173	1.9278	2.0122	1.4195	1.5888	1.5887	1.7514	1.8448	1.9585
BS 2	0.6518	0.8394	0.6859	0.7325	0.7224	0.8514	0.7032	0.6667	0.7249	0.7673
Node B	0.0632	0.0803	0.0656	0.0616	0.1238	0.0936	0.0945	0.0771	0.0710	0.0643
eNode B	3.0044	2.1513	2.7918	2.4993	2.4442	2.0899	2.6933	2.9675	2.6000	2.3685
AP 1	0.0102	0.0427	0.0179	0.0133	0.0055	0.0155	0.0226	0.0295	0.0659	0.0198
AP 2	0.0058	0.0287	0.0098	0.0160	0.0022	0.0072	0.0048	0.0065	0.0206	0.0409
AP 3	0.0037	0.0814	0.0051	0.0048	0.0080	0.1914	0.0165	0.0076	0.0098	0.0068
AP 4	0.0070	0.0108	0.0091	0.0056	0.0100	0.0100	0.2311	0.0413	0.0152	0.0064
AP 5	0.0578	0.0092	0.2349	0.0318	0.0030	0.0050	0.0094	0.0574	0.1557	0.0271
TV Tower 1	0.1277	0.1265	0.1275	0.1279	0.1246	0.1257	0.1257	0.1267	0.1271	0.1277
TV Tower 2	0.1220	0.1237	0.1224	0.1229	0.1228	0.1238	0.1225	0.1221	0.1227	0.1232
TV Tower 3	0.1185	0.1197	0.1187	0.1183	0.1215	0.1204	0.1204	0.1195	0.1191	0.1186
TV Tower 4	0.1172	0.1156	0.1168	0.1164	0.1164	0.1155	0.1167	0.1171	0.1165	0.1161
Total Energy	6.2534	5.4466	6.2333	5.8626	5.2239	5.3382	5.8494	6.0904	5.9933	5.7452

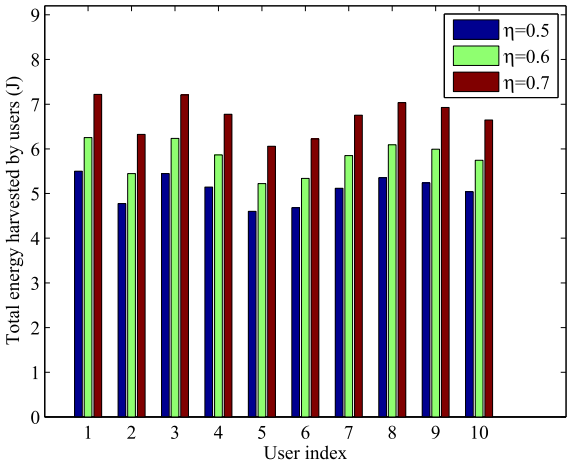

FIGURE 5. Total energy harvested by each user under different energy harvesting efficiencies.

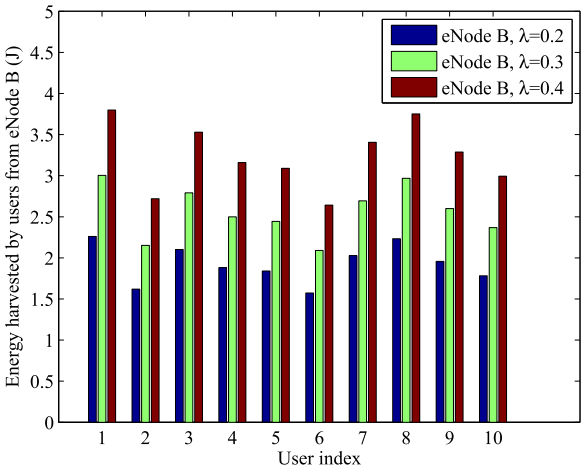

FIGURE 6. Energy harvested by each user from eNode B under different service arrival rates.

In addition, Fig. 5 shows the total energy harvested by each user under different energy harvesting efficiencies. It can be observed that the total energy harvested by each user increases with the growth of the energy harvesting efficiency from 0.5 to 0.7. The higher the energy harvesting efficiency is, the more electrical energy can be obtained by converting RF signals into DC voltage. Fig. 6 reveals the energy harvested by each user from eNode B under different service arrival rates. We can find that the energy harvested by each user grows gradually as the service arrival rate increases from 0.2 to 0.4. For the ambient transmitter eNode B, it will communicate with more users under a higher service arrival rate. That is to say the eNode B will transmit more power. Therefore, each user can harvest more energy from the received electromagnetic waves.

C. CONVERGENCE AND TIME COMPLEXITY OF QPSO ALGORITHM

In this subsection, the convergence and time complexity of the QPSO algorithm are discussed. In the simulations, the number of sub-carriers is set as 80. Fig. 7 illustrates the convergence of the QPSO algorithm under different numbers of particles. It can be observed that the energy efficiency rises up gradually as the number of iterations increases. When the number of iterations is 350, the energy efficiency tends to be stable. Besides, the energy efficiency increases progressively with the growth of the number of particles from 5 to 30. The reason is that a more accurate suboptimal solution can be obtained with more particles. However, the growth rate of the energy efficiency is reduced to some extent. Consequently, the number of iterations and the number of particles are set as 350 and 30 in the following sets of simulations.

Fig. 8 evaluates the time complexity of the QPSO algorithm under different numbers of particles from the perspective of average CPU time. We can see that the average CPU time increases as the number of iterations increases. At the same time, the increase rate of the average CPU time goes up gradually as the number of particles grows from 5 to 30. That is because each particle needs to update its position based on the position update equation. The position of each particle is a

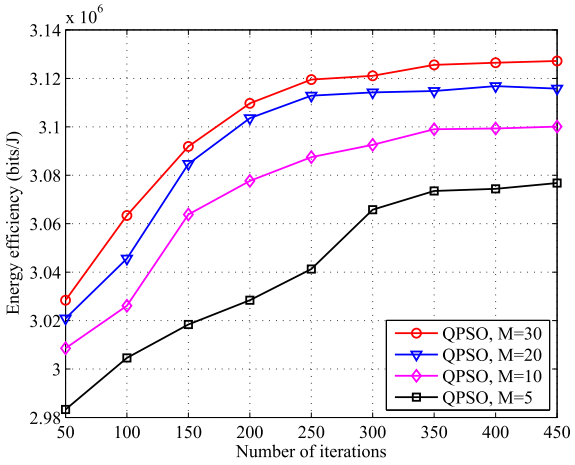

FIGURE 7. Energy efficiency versus number of iterations with $K = 10$.

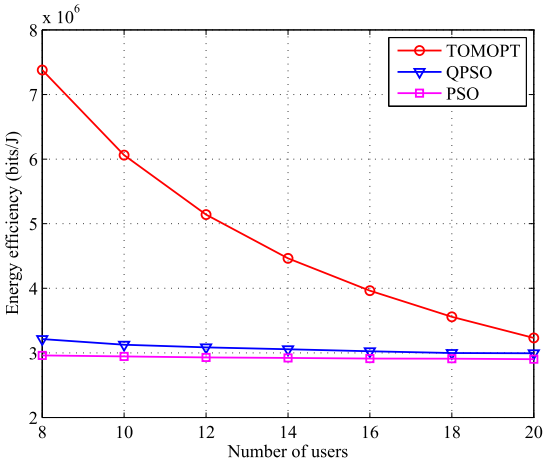

FIGURE 9. Energy efficiency versus number of users with $N = 80$.

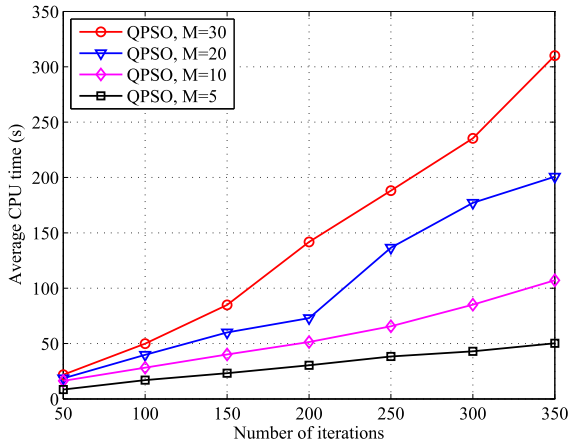

FIGURE 8. Average CPU time versus number of iterations with $K = 10$.

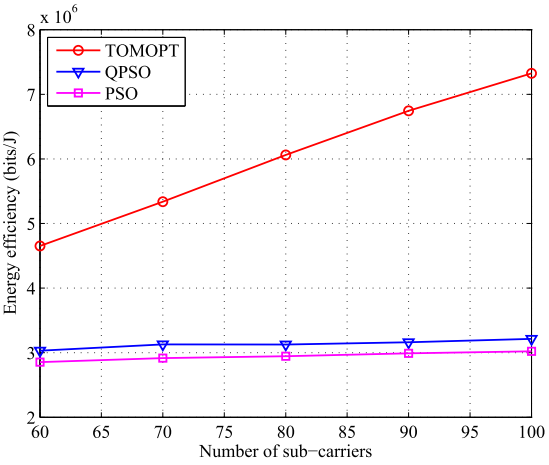

FIGURE 10. Energy efficiency versus number of sub-carriers with $K = 10$.

multi-dimensional vector. A larger number of particles results in more time spent in updating the positions.

D. PERFORMANCE COMPARISONS

In this subsection, some simulation results are shown to compare the proposed resource allocation strategy with traditional methods. An existing resource allocation strategy based on the PSO [40] is used for comparison. Meanwhile, TOMLAB optimization (TOMOPT) environment [46], which is developed by the TOMLAB Optimization Incorporation, is adopted to obtain the optimal solution to the MINLP problem in (8).

Fig. 9 depicts the relationship between the energy efficiency and the number of users under the TOMOPT, QPSO, and PSO methods. We can find that the energy efficiency decreases with the growth of the number of users from 8 to 20. That is because more total energy is consumed. The growth rate of the total energy consumption is higher than that of the amount of total data. In addition, the QPSO method has lower energy efficiency than the optimal TOMOPT method and higher energy efficiency than the PSO method. It can be explained that the QPSO method can obtain a globally suboptimal solution while the PSO method is easy to fall into a locally optimal solution. Meanwhile, the TOMOPT approach has much faster decrease rate of the energy efficiency than the QPSO and PSO methods. Therefore, the energy efficiency gap between the optimal TOMOPT approach and the QPSO and the PSO methods decreases gradually as the number of users increases.

Fig. 10 presents the relationship between the energy efficiency and the number of sub-carriers under the TOMOPT, QPSO, and PSO methods. We can observe that the energy efficiency rises up as the number of sub-carriers increases from 60 to 100. The reason is that more data can be delivered. The growth rate of the amount of total data is higher than that of the total energy consumption. Similarly, although the QPSO method is inferior to the optimal TOMOPT approach, it is superior to the PSO method. The reason is the same as that in Fig. 9. Furthermore, the TOMOPT approach has much faster increase rate of the energy efficiency than the QPSO and PSO methods. Consequently, the energy efficiency gap between the optimal TOMOPT approach and the QPSO and

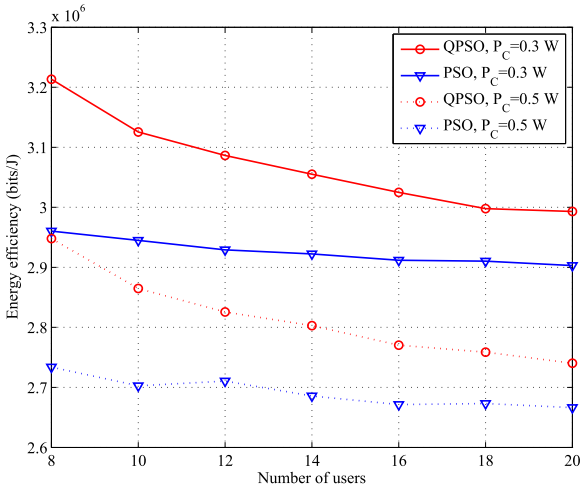

FIGURE 11. Energy efficiency versus number of users under different circuit power consumption with $N = 80$.

the PSO methods increases gradually as the number of sub-carriers increases.

Fig. 11 compares the performance of the energy efficiency between the QPSO method and the PSO approach under different circuit power consumption. A similar variation trend about the energy efficiency versus the number of users can be found. The QPSO method always outperforms the PSO approach. Furthermore, it can be seen that the energy efficiency descends with the increase of the circuit power consumption from 0.3 W to 0.5 W for obvious reasons.

V. CONCLUSIONS

In this paper, an energy-efficient sub-carrier and power allocation strategy has been proposed in a cloud-based cellular network with ambient RF energy harvesting. By employing a broadband rectenna, each user can harvest ambient RF energy over six frequency bands simultaneously. Taking service arrival in different ambient transmitters into account, a novel energy arrival model has been presented. The resource allocation problem has been formulated as a MINLP problem. The suboptimal solution has been achieved by introducing the QPSO method. Simulation results have shown that the QPSO approach can obtain higher energy efficiency than the PSO method. We assume that the users are stationary in this work. In a practical cloud-based cellular network, users are usually in motion. Therefore, in our future work we shall consider energy harvesting mobile users based on some mobility model. We shall further replace the simple channel gain model used in this paper with a more realistic fading channel model. In addition, we shall also take into consideration of the user devices as ambient RF sources, by modifying the energy arrival model accordingly. We shall also generalize the single BS scenario considered in this paper by considering heterogeneous networking scenarios with macro-, micro-, pico-, and femto-BSs.

REFERENCES

[1] C. Zhu, V. C. M. Leung, X. Hu, L. Shu, and L. T. Yang, "A review of key issues that concern the feasibility of mobile cloud computing," in *Proc. IEEE Int. Conf., IEEE Cybern., Phys., Soc. Comput.*, Aug. 2013, pp. 769–776.

[2] C. Zhu, V. C. M. Leung, L. T. Yang, and L. Shu, "Collaborative location-based sleep scheduling for wireless sensor networks integrated with mobile cloud computing," *IEEE Trans. Comput.*, vol. 64, no. 7, pp. 1844–1856, Jul. 2015.

[3] C. Zhu, Z. Sheng, V. C. M. Leung, L. Shu, and L. T. Yang, "Towards offering more useful data reliably to mobile cloud from wireless sensor network," *IEEE Trans. Emerg. Topics Comput.*, vol. 3, no. 1, pp. 84–94, Mar. 2015.

[4] C. Zhu, H. Wang, X. Liu, L. Shu, L. T. Yang, and V. C. M. Leung, "A novel sensory data processing framework to integrate sensor networks with mobile cloud," *IEEE Syst. J.*, vol. 10, no. 3, pp. 1125–1136, Sep. 2016.

[5] A. R. Khan, M. Othman, S. A. Madani, and S. U. Khan, "A survey of mobile cloud computing application models," *IEEE Commun. Surveys Tuts.*, vol. 16, no. 1, pp. 393–413, 1st Quart., 2014.

[6] P. Shu, F. Liu, H. Jin, M. Chen, F. Wen, and Y. Qu, "eTime: Energy-efficient transmission between cloud and mobile devices," in *Proc. IEEE INFOCOM*, Turin, Italy, Apr. 2013, pp. 195–199.

[7] G. Han, W. Que, G. Jia, and L. Shu, "An efficient virtual machine consolidation scheme for multimedia cloud computing," *Sensors*, vol. 16, no. 2, pp. 1–17, Feb. 2016.

[8] G. Han, J. Jiang, M. Guizani, and J. J. P. C. Rodrigues, "Green routing protocols for wireless multimedia sensor networks," *Sensors*, vol. 23, no. 6, pp. 140–146, Dec. 2016.

[9] G. Jia, G. Han, J. Jiang, and L. Liu, "Dynamic adaptive replacement policy in shared last-level cache of DRAM/PCM hybrid memory for big data storage," *IEEE Trans. Ind. Informat.*, to be published.

[10] C. You, K. Huang, and H. Chae, "Energy efficient mobile cloud computing powered by wireless energy transfer," *IEEE J. Sel. Areas Commun.*, vol. 34, no. 5, pp. 1757–1771, May 2016.

[11] K. Huang and V. K. N. Lau, "Enabling wireless power transfer in cellular networks: Architecture, modeling and deployment," *IEEE Trans. Wireless Commun.*, vol. 13, no. 2, pp. 902–912, Feb. 2014.

[12] H. Ju and R. Zhang, "Throughput maximization in wireless powered communication networks," *IEEE Trans. Wireless Commun.*, vol. 13, no. 1, pp. 418–428, Jan. 2014.

[13] I. Krikidis, S. Timotheou, S. Nikolaou, G. Zheng, D. W. K. Ng, and R. Schober, "Simultaneous wireless information and power transfer in modern communication systems," *IEEE Commun. Mag.*, vol. 52, no. 11, pp. 104–110, Nov. 2014.

[14] D. W. K. Ng, E. S. Lo, and R. Schober, "Wireless information and power transfer: Energy efficiency optimization in OFDMA systems," *IEEE Trans. Wireless Commun.*, vol. 12, no. 12, pp. 6352–6370, Dec. 2013.

[15] C. Xiong, L. Lu, and G. Y. Li, "Energy efficiency tradeoff in downlink and uplink TDD OFDMA with simultaneous wireless information and power transfer," in *Proc. IEEE Int. Conf. Commun.*, Jun. 2014, pp. 1–6.

[16] R. Morsi, D. S. Michalopoulos, and R. Schober, "Multiuser scheduling schemes for simultaneous wireless information and power transfer over fading channels," *IEEE Trans. Wireless Commun.*, vol. 14, no. 4, pp. 1967–1982, Apr. 2015.

[17] E. Boshkovska, D. W. K. Ng, N. Zlatanov, and R. Schober, "Practical non-linear energy harvesting model and resource allocation for SWIPT systems," *IEEE Commun. Lett.*, vol. 19, no. 12, pp. 2082–2085, Dec. 2015.

[18] J. A. Hagerty, F. B. Helmbrecht, W. H. McCalpin, R. Zane, and Z. B. Popovic, "Recycling ambient microwave energy with broad-band rectenna arrays," *IEEE Trans. Microw. Theory Techn.*, vol. 52, no. 3, pp. 1014–1024, Mar. 2004.

[19] C. Song, Y. Huang, J. Zhou, S. Yuan, Q. Xu, and P. Carter, "A broadband efficient rectenna array for wireless energy harvesting," in *Proc. 9th Eur. Conf. Antennas Propag.*, Apr. 2015, pp. 1–5.

[20] Z. Liu, Z. Zhong, and Y. X. Guo, "Enhanced dual-band ambient RF energy harvesting with ultra-wide power range," *IEEE Microw. Wireless Compon. Lett.*, vol. 25, no. 9, pp. 630–632, Sep. 2015.

[21] S. Keyrouz, H. J. Visser, and A. G. Tijhuis, "Multi-band simultaneous radio frequency energy harvesting," in *Proc. 7th Eur. Conf. Antennas Propag.*, Apr. 2013, pp. 3058–3061.

[22] C. Song, Y. Huang, J. Zhou, J. Zhang, S. Yuan, and P. Carter, "A high-efficiency broadband rectenna for ambient wireless energy harvesting," *IEEE Trans. Antennas Propag.*, vol. 63, no. 8, pp. 3486–3495, Aug. 2015.

[23] V. Kuhn *et al.*, "A multi-band stacked RF energy harvester with RF-to-DC efficiency up to 84%," *IEEE Trans. Microw. Theory Techn.*, vol. 63, no. 5, pp. 1768–1778, May 2015.

[24] C. Song *et al.*, "A novel six-band dual CP rectenna using improved impedance matching technique for ambient RF energy harvesting," *IEEE Trans. Antennas Propag.*, vol. 64, no. 7, pp. 3160–3171, Jul. 2016.

[25] I. Flint, X. Lu, N. Privault, D. Niyato, and P. Wang, "Performance analysis of ambient RF energy harvesting with repulsive point process modeling," *IEEE Trans. Wireless Commun.*, vol. 14, no. 10, pp. 5402–5416, Oct. 2015.

[26] X. Lu, I. Flint, D. Niyato, N. Privault, and P. Wang, "Performance analysis of simultaneous wireless information and power transfer with ambient RF energy harvesting," in *Proc. IEEE Wireless Commun. Netw. Conf.*, Mar. 2015, pp. 1303–1308.

[27] X. Lu, P. Wang, D. Niyato, and Z. Han, "Resource allocation in wireless networks with RF energy harvesting and transfer," *IEEE Netw.*, vol. 29, no. 6, pp. 68–75, Nov.-Dec. 2015.

[28] J. Sun, W. Xu, and F. Bin, "A global search strategy of quantum-behaved particle swarm optimization," in *Proc. IEEE Conf. Cybern. Intell. Syst.*, Dec. 2004, pp. 111–116.

[29] H. Yuan, Y. Wang, and L. Chen, "An availability-aware task scheduling for heterogeneous systems using quantum-behaved particle swarm optimization," in *Proc. Int. Conf. Swarm Intell.*, Jun. 2010, pp. 120–127.

[30] J. Sun, W. Fang, X. Wu, V. Palade, and W. Xu, "Quantum-behaved particle swarm optimization: Analysis of individual particle behavior and parameter selection," *Evol. Comput.*, vol. 20, no. 3, pp. 349–393, Sep. 2012.

[31] Y. Zhao, X. Li, Y. Li, and H. Ji, "Resource allocation for high-speed railway downlink MIMO-OFDM system using quantum-behaved particle swarm optimization," in *Proc. IEEE Int. Conf. Commun. (ICC)*, Jun. 2013, pp. 2343–2347.

[32] *User Equipment (UE) Radio Transmission and Reception*, document TS 36.101 version 10.3.0, 3GPP, Jun. 2011.

[33] H. J. Visser and R. J. M. Vullers, "RF energy harvesting and transport for wireless sensor network applications: Principles and requirements," *Proc. IEEE*, vol. 101, no. 6, pp. 1410–1423, Jun. 2013.

[34] X. Lu, P. Wang, D. Niyato, D. I. Kim, and Z. Han, "Wireless network with RF energy harvesting: A contemporary survey," *IEEE Commun. Surveys Tuts.*, vol. 17, no. 2, pp. 757–789, 2nd Quart., 2015.

[35] C. W. Leong, W. Zhuang, Y. Cheng, and L. Wang, "Optimal resource allocation and adaptive call admission control for voice/data integrated cellular networks," *IEEE Trans. Veh. Technol.*, vol. 55, no. 2, pp. 654–669, Mar. 2006.

[36] H. Gao, T. Lv, W. Wang, and N. C. Beaulieu, "Energy-efficient and secure beamforming for self-sustainable relay-aided multicast networks," *IEEE Signal Process. Lett.*, vol. 23, no. 11, pp. 1509–1513, Nov. 2016.

[37] H. Gao, T. Lv, X. Su, H. Yang, and J. M. Cioffi, "Energy-efficient resource allocation for massive MIMO amplify-and-forward relay systems," *IEEE Access*, vol. 4, pp. 2771–2787, May 2016.

[38] J. Kennedy and R. Eberhart, "Particle swarm optimization," in *Proc. IEEE Int. Conf. Neural Netw.*, Nov./Dec. 1995, pp. 1942–1948.

[39] R. Poli, J. Kennedy, and T. Blackwell, "Particle swarm optimization: An overview," *Swarm Intell.*, vol. 1, no. 1, pp. 33–57, 2007.

[40] Y. Shi and R. Eberhart, "A modified particle swarm optimizer," in *Proc. IEEE Int. Conf. Evol. Comput., IEEE World Congr. Comput. Intell.*, Anchorage, AK, USA, May 1998, pp. 69–73.

[41] D. Sen, "The uncertainty relations in quantum mechanics," *Current Sci.*, vol. 107, no. 2, pp. 203–218, Jul. 2014.

[42] *Radio Transmission and Reception*, document GSM 05.05 Version 5.2.0, ETSI, Jul. 1996.

[43] *Base Station (BS) Radio Transmission and Reception (FDD)*, document TS 25.104 version 6.17.0, 3GPP, Apr. 2008.

[44] *Radio Frequency (RF) System Scenarios* document TR 36.942 version 10.2.0, 3GPP, May 2011.

[45] *Background for Radio Frequency (RF) Requirements*, document GSM 05.50 version 6.1.0, 3GPP, Apr. 2000.

[46] K. Holmstrom, A. O. Goran, and M. M. Edvall, *User's Guide for TOMLAB 7*, Seattle, WA, USA: TOMLAB Optim. Incorporat., May 2010.

YISHENG ZHAO (M'16) received the B.Eng. degree in communication engineering from Anhui Normal University, China, in 2006, the M.Eng. degree in communication and information system from the Chongqing University of Posts and Telecommunications, China, in 2010, and the Ph.D. degree in communication and information system from the Beijing University of Posts and Telecommunications, China, in 2013. He is currently an Assistant Professor with the College of Physics and Information Engineering, Fuzhou University, China. He is also a Visiting Scholar with the Department of Electrical and Computer Engineering, The University of British Columbia, Canada. His research interests include energy harvesting communications, mobile cloud computing, radio resource management, and channel prediction.

VICTOR C. M. LEUNG (S'75–M'89–SM'97–F'03) received the B.A.Sc. degree (hons.) in electrical engineering and the Ph.D. degree in electrical engineering from The University of British Columbia (UBC) in 1977 and 1982, respectively.

He attended graduate school with UBC on a Canadian Natural Sciences and Engineering Research Council Postgraduate Scholarship. From 1981 to 1987, he was a Senior Member of Technical Staff and Satellite System Specialist with MPR Teltech Ltd., Canada. In 1988, he was a Lecturer with the Department of Electronics, The Chinese University of Hong Kong. He was with UBC as a Faculty Member in 1989, and currently holds the positions of Professor and the TELUS Mobility Research Chair in advanced telecommunications engineering with the Department of Electrical and Computer Engineering. He has co-authored over 950 technical papers in international journals and conference proceedings, 37 book chapters, and co-edited 12 book titles. Several of his papers had been selected for best paper awards. His research interests are in the areas wireless networks and mobile systems.

Dr. Leung is a registered Professional Engineer in the Province of British Columbia, Canada. He is a Fellow of the Royal Society of Canada, the Engineering Institute of Canada, and the Canadian Academy of Engineering. He was a recipient of the IEEE Vancouver Section Centennial Award and the 2012 UBC Killam Research Prize. He received the APEBC Gold Medal as the Head of the graduating class with the Faculty of Applied Science. He was a Distinguished Lecturer of the IEEE Communications Society. He is serving on the Editorial Board of the IEEE Wireless Communications Letters, the IEEE Transactions on Green Communications and Networking, the IEEE Access, the *Computer Communications*, and several other journals, and has previously served on the editorial boards of the IEEE Journal on Selected Areas in Communications–Wireless Communications Series and Series on Green Communications and Networking, the IEEE Transactions on Wireless Communications, the IEEE Transactions on Vehicular Technology, the IEEE Transactions on Computers, and the Journal of Communications and Networks. He has guest-edited many journal special issues, and provided leadership to the organizing committees and technical program committees of numerous conferences and workshops.

CHUNSHENG ZHU (S'12–M'16) received the B.E. degree in network engineering from the Dalian University of Technology, China, in 2010, the M.Sc. degree in computer science from St. Francis Xavier University, Canada, in 2012, and the Ph.D. degree in electrical and computer engineering from The University of British Columbia, Canada, in 2016. He is currently a Post-Doctoral Research Fellow with the Department of Electrical and Computer Engineering, The University of British Columbia. He has authored over 80 papers published or accepted by refereed international journals/magazines including the IEEE TRANSACTIONS ON INDUSTRIAL ELECTRONICS, the IEEE TRANSACTIONS ON COMPUTERS, the IEEE TRANSACTIONS ON INFORMATION FORENSICS AND SECURITY, the IEEE TRANSACTIONS ON EMERGING TOPICS IN COMPUTING, the IEEE TRANSACTIONS ON CLOUD COMPUTING, the IEEE SYSTEMS JOURNAL, the IEEE ACCESS, and the *IEEE Communications Magazine* and conferences, including the IEEE Globecom and the IEEE ICC. His current research interests mainly include wireless sensor networks, cloud computing, Internet of Things, social networks, and security.

HUI GAO (S'10–M'13–SM'16) received the B.Eng. degree in information engineering and the Ph.D. degree in signal and information processing from the Beijing University of Posts and Telecommunications (BUPT), Beijing, China, in 2007 and 2012, respectively. From 2009 to 2012, he served as a Research Assistant with the Wireless and Mobile Communications Technology Research and Development Center, Tsinghua University, Beijing. In 2012, he visited the Singapore University of Technology and Design (SUTD), Singapore, as a Research Assistant. From 2012 to 2014, he was a Post-Doctoral Researcher with SUTD. He is currently with the School of Information and Communication Engineering, BUPT, as an Associate Professor. His research interests include massive MIMO systems, cooperative communications, ultra wideband wireless communications, and energy efficient wireless communications.

ZHONGHUI CHEN received the B.Eng. degree in electronic engineering from Xidian University, China, in 1982, and the M.Eng. degree in communication and electronic systems from Tsinghua University, China, in 1984. He is currently a Professor with the College of Physics and Information Engineering, Fuzhou University, China. He is also the Director of the Department of Communication Engineering. His research interests include Internet of vehicles, power line communications, and wireless communications and networks.

HONG JI (SM'09) received the B.S. degree in communications engineering and the M.S. and Ph.D. degrees in information and communications engineering from the Beijing University of Posts and Telecommunications (BUPT), Beijing, China, in 1989, 1992, and 2002, respectively. In 2006, she was a Visiting Scholar with The University of British Columbia, Vancouver, BC, Canada. She is currently a Professor with the School of Information and Communication Engineering, BUPT. Her research interests include wireless networks and mobile systems, ICT applications, system architectures, cloud computing, software defined networks, network function virtualization, radio access, protocols, management algorithms, performance evaluations.

Dr. Ji has served on the Technical Program Committees (TPCs) of numerous conferences, such as the IEEE International Conference on Communications, the IEEE Global Communications Conference, the IEEE WIRELESS COMMUNICATIONS AND NETWORKING Conference, the IEEE International Conference on Computer Communications workshops, and the IEEE International Conference on Computer, Information, and Telecommunication Systems. She has also served as a TPC Co-chair for the 2011 International Conference on Communications and Networking in China workshops and as a Program Co-chair for the 2012-2014 International Conference on Wireless Information Networks and Systems. She serves on the Editorial Board of several journals, including the IEEE TRANSACTIONS ON GREEN COMMUNICATIONS AND NETWORKING AND MOBILE COMPUTING and the Wiley *International Journal of Communication Systems*.